Journal of Otpoelectronics and Advanced Materials Vol. 7, No. 5, October 2005, p. 2267 - 2273

NANOSTRUCTURAL VOIDS IN GLASSY-LIKE As_2Se_3 STUDIED WITH FSDP-RELATED XRD AND PALS TECHNIQUES

T. S. Kavetskyy[a,b], O. I. Shpotyuk[b,c*]

[a]Solid-State Microelectronics Laboratory, Drohobych Ivan Franko State Pedagogical University, 24, Franko str., Drohobych, 82100, Ukraine
[b]Institute of Materials, Scientific Research Company “Carat”, 202, Stryjska str., Lviv, 79031, Ukraine
[c]Institute of Physics, Jan Dlugosz University of Czestochowa, 13/15, al. Armii Krajowej, Czestochowa, 42201, Poland

Nanostructural voids in glassy-like As_2Se_3 have been studied using X-ray diffraction in respect to the first sharp diffraction peak (FSDP-related XRD) within well-known Elliott’s void-based model for the origin of the FSDP and positron annihilation lifetime spectroscopy (PALS). A good agreement between experimental data and theoretical ones obtained within Popescu’s model for nanovoid distribution in glass structural network has been observed. The empirical relationship between the position of the FSDP and diameter of nanovoids has been established for the investigated layer-like type chalcogenide glass for the first time. The perspectives in using of FSDP-related XRD along with PALS for research of nanoscale void-species structure in network chalcogenide glasses have been demonstrated.

(Received August 24, 2005; accepted September 22, 2005)

Keywords: Chalcogenide glasses, Positron annihilation, X-ray diffraction, First sharp diffraction peak

1. Introduction

Despite recent progress in practical application of chalcogenide glasses in various fields of modern optoelectronics [1-5], their structural features and, consequently, physical properties need still more understanding and detail research. It is connected, first of all, that ChG with essential excess of free volume in comparison to thermodynamic equilibrium crystals (see Fig. 1), along with atomic species structure, are characterized by void-species one (internal structural nanovoids), formed technologically during melt quenching procedure.

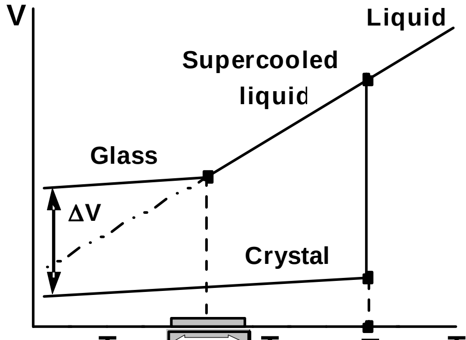

Fig. 1. $T(V)$ diagram showing excess of free volume (ΔV) for glass in comparison with thermodynamic equilibrium crystal of the same chemical composition (T_g – glass transition temperature, T_m – melting point).

---

[*] Corresponding author: shpotyuk@novas.lviv.ua

Indeed, a number of works [6-10] confirm a key role of free volume in structural changes stimulated by external influences (pressure, photoexposure, radiation, etc.). To date, however, researchers operate by only parameters of free volume, such as, for instance, compactness of glass structure δ [7,8] which is a measure of free volume, whereas the information concerning topological features and size of nanovoids which form the free volume in ChG network remains still open.

In terms of S.R. Elliott [11], atomic-species structure in ChG on the level of the nearest inter-atomic correlations (so-called nanoscale or nanostructural level) is described by (i) *short-range order (ShRO)* in atomic arrangement (~ 0.2-0.5 nm), defined via coordination number for the chosen central atom, average covalent bond distances and Debye-Waller disorder factors for the first and all following coordination shells, main types of structural units in a glassy-like network, etc.; (ii) *medium-range order (MRO)* in atomic arrangement, three sub-levels being distinguished in dependence on inter-atomic length scale: near-MRO (~0.5 nm) in connection between individual coordination polyhedra (corner-, edge- or face-sharing structural units), intermediate-MRO (0.5-0.8 nm) in well-defined orientations in mutually-interconnected coordination polyhedra (super-structural units) and far-MRO (0.8-2.0 nm) in local dimensionality of covalent-bonded glass network; and (iii) *long-range order (LRO)* in atomic arrangement within whole glass bulk (> 2.0 nm) is typically absent in ChG, but, sometimes, LRO is associated with microscopic inhomogeneities and large-scale imperfections (second-phase extractions, column-grown morphology, microcrystallites, etc.).

These above nanoscale levels in void-species structure would be also attributed to the corresponding nanovoids. So, *the lowest (first) level of structural organisation (SRO)* in void-species structure can be attributed to the smallest nanovoids formed by atomic fluctuations frozen technologically at melt quenching (quasi-network fluctuational nanovoids) and stereometric specificity in local bond-charge density distribution around individual ChG-forming atoms, their typical radii being no more than 0.1-0.2 nm. The latter nanovoids, in terms of M.A. Kastner [12], are formed by bond-free solid angles (BFSA) in covalent-linked glass network. The spatially-stretched nanovolume voids between interconnected topologically-inconsistent structural units within glass-forming network (~0.2-0.3 nm in radius) or, in other words, geometrical nanovoids represent *the next higher (second or intermediate) level of structural organisation (MRO)* in void-species structure of ChG. And *the highest (third) level of structural organisation (LRO)* in void-species structure is attributed to microvolume voids and void-like imperfections with radii more than ~0.3 nm in glass bulk (intrinsic cracks, strained knags and bubble-like inclusions, etc.).

The idea to study nanovoid topology features in glass network has firstly been proposed by M. A. Popescu yet in the early 80-s in respect to the void structure of computer models of amorphous solids including random and layer-biased a-As_2Se_3 [13], but it was not accepted entirely because of lack of corresponding experimental confirmations. Moreover, the well-known announcement of S. G. Bishop and N. J. Shevchik from 1974 [14], declaring the absence of atomic free-volume voids with detectable radius more than 3 Å at the volume fraction above 1 % in ChG, testifies rather in a favour of its meaninglessness.

Furthermore (in 1991-1995), S. R. Elliott [11,15,16], interpreting the nature of the anomalous first sharp diffraction peak (FSDP) as a chemical-order prepeak in the concentration-concentration structure factor, arising from the clustering of interstitial nanovoids around cation-based structural units, has proposed and tested for AX_2-type glassy-like materials (e.g. $GeS(Se)_2$) the empirical relationship between the position of the FSDP, Q_1, and atom-void separation like to diameter of nanovoids, D:

$$Q_1 = 3\pi/2D. \tag{1}$$

The Eq. (1), apparently, testifies that FSDP-related XRD can be adequate experimental tool to obtain information concerning size of nanovoids in the real glass network. It is understood, however, that Eq. (1) can not be applied for non-crystalline materials another type structure, namely ChG with layer-like type structure based on the $AsX_{3/2}$ structural units. Thus, actual task will be to found such correlations for these type materials.

Positron annihilation technique would be also served as an alternative experimental tool in this direction. This method has been examined in 1995 by K.O. Jensen with co-workers [17] for layer-like type ChG on the example of As_2Se_3. So, demonstrating the model of positron traps by vacancy-like defects, it has been found the linear regularity between positron lifetime τ (in ns) and vacancy volume V (in Å^3) accordingly to the next expression:

$$\tau \cong 0.240 + 0.0013 \cdot V. \tag{2}$$

Besides, in Ref. [17], authors have firstly suggested that the positron lifetime method might provide a sensitive test of the Elliott's model for the FSDP in the total structure factor of network ChG, assuming therefore that the same nanovoids can be responsible for positron trapping and origin of the FSDP. Nevertheless, no experimental test of this suggestion has been made in the research as well as modification of the Elliott's model for layer-like g-As_2Se_3.

It is significantly that study of local structure of liquid and glassy As_2Se_3 using anomalous X-ray scattering method [18] confirms also the main principles of the Elliott model for the FSDP in the case of tetravalent ChG, but, as it was noted, more detail investigation and discussion for layer-like glassy As_2Se_3 is still required.

According to P.H. Gaskell [19], the fact that voids, rings, and quasi-lattice planes are all useful descriptors of medium-range structure, can serve as an additional confirmation for the Elliott's approach for the FSDP.

In the recent papers [20,21] Popescu et al. have shown that closed cluster model of As_2S_3 glasses is able to explain some features of FSDP, on the basis of the packing of clusters with the inclusion of voids. Therefore, nanostructural void characterization for layer-like type ChG is an actual problem now.

Combination of the FSDP-related XRD along with PALS seems to be reasonable to resolve such task. In the present work the experimental results obtained in this direction have firstly been demonstrated for g-As_2Se_3 as an example.

2. Experimental

Two identical samples of *g*-As_2Se_3 prepared by a standard melt-quenching procedure were used for research. Ampoules synthesized were quenched in water. Before experimental measurements samples were polished to the ~1.5 mm thickness disks of optical quality and annealed near 20-30 K below glass transition temperature T_g.

XRD pattern was obtained using HZG-4a powder diffractometer with Cu K_α-radiation. Diffraction data were collected in the range of $10 \leq 2\theta \leq 40°$ (a step of 0.05° and an integration time of 70 sec per point). The sample was measured in the regime of "rotation" (speed of 2 rotations per sec). The program CSD (Crystal Structure Determination) „Full profile powder data reduction" V.5.11 was used for data treatment. The 2θ error in determining the position was ± 0.01°.

According to the Elliott's void-based model for the origin of the FSDP [16], the FSDP parameters, such as the interlayer separation, quasi-periodic in nature with an effective periodicity, *R*, and correlation length, *L*, over which quasi-periodic real-space density fluctuations take place, were calculated, respectively, as

$$R \approx 2\pi / Q_1, \tag{3}$$

and

$$L \approx 2\pi / \Delta Q_1, \tag{4}$$

where the magnitude of the scattering vector Q_1 ($= 4\pi \sin\theta / \lambda$) corresponds to the position of the FSDP and ΔQ_1 is the full width at half maximum (FWHM) of the FSDP.

The PALS experiment was performed using an ORTEC spectrometer with ^{22}Na source placed between two sandwiched *g*-As_2Se_3 samples [22]. The data obtained were mathematically treated with LT computer program [23]. The *FIT* value was determined as statistically weighted least-squares deviation between experimental and theoretical data using expression:

$$FIT = \frac{\sum_{k=1}^{N} \left(\frac{T_k - E_k}{\sqrt{E_k}} \right)^2}{N - m} \approx \frac{1}{N} \sum_{k=1}^{N} \left(\frac{T_k - E_k}{\sqrt{E_k}} \right), \tag{5}$$

where N is number of channels, E_k is experimentally measured number of counts in the channel No k, T_k is theoretical number of counts in the channel No k, $\sqrt{E_k}$ is standard deviation for count number in the channel No k, m - number of fitting parameters. The optimal *FIT* values were taken to be quite close to 1.0, where the normal deviation range of *FIT* is 0.95 ÷ 1.10. The best PALS results within two-state positron trapping model [24] were corresponded to two-component fitting procedure, giving τ_1, τ_2, I_1 and I_2 values (where τ_1 – reduced bulk lifetime, τ_2 – defect-related lifetime, associated with nanovoid volume, I_1 and I_2 – corresponding lifetime intensities ($I_1 + I_2 = 1$, and I_2 values testify about concentration of nanovoids in glass matrix). On the basis of τ_1, τ_2, I_1 and I_2 values obtained with applied fitting procedure, the numerical parameters of this model, such as bulk positron lifetime τ_B, average positron lifetime $\bar{\tau}$ and positron trapping rate k_d, were respectively calculated using formula:

$$\tau_B = \left(\frac{I_1}{\tau_1} + \frac{I_2}{\tau_2} \right)^{-1} = \frac{\tau_1 \tau_2}{I_1 \tau_2 + I_2 \tau_1}, \tag{6}$$

$$\bar{\tau} = I_1 \tau_1 + I_2 \tau_2, \tag{7}$$

$$k_d = I_2 \left(\frac{1}{\tau_1} - \frac{1}{\tau_2} \right). \tag{8}$$

3. Results and discussion

Fig. 2 shows the XRD pattern for g-As_2Se_3 and Table 1 demonstrates the CSD program treatment of the XRD data obtained and FSDP parameters calculated within the Elliott's model [16].

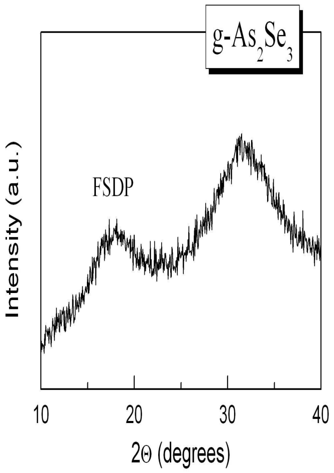

Fig. 2. X-ray diffraction pattern (Cu K_α-radiation) for g-As_2Se_3.

The FSDP for g-As_2Se_3 is around $2\theta = 17.67°$ that correspond to the scattering vector $Q_1 = Q_{FSDP} \cong 1.25$ Å^{-1}. The magnitude of FWHM of the FSDP is equal to 4.88° or $\Delta Q_1 \cong 0.35$ Å^{-1}. The interlayer separation with an effective periodicity, R (the atom-void distance in terms of Elliott's void-based model [16]), and correlation length, L, calculated according to Eqs. (3) and (4), are found nearby 5.03 Å and 17.9 Å, respectively. It means that periodicity of $R \cong 5.03$ Å is necessary to give the FSDP at the observed value of $Q_1 \cong 1.25$ Å^{-1} and this real-space quasi-periodicity takes place along the correlation length of $L \cong 17.9$ Å.

Table 1. The FSDP parameters obtained within the Elliott's void-based model [16] for g-As_2Se_3.

2θ (°)	$\pm 2\theta$ (°)	Q_1 (Å^{-1})	FWHM (°)
17.67	0.01	1.25	4.88
± FWHM (°)	ΔQ_1 (Å^{-1})	R (Å)	L (Å)
0.05	0.35	5.03	17.9

The most real PALS characteristics with the optimal *FIT* range of 0.95÷1.10, proper to the examined g-As_2Se_3 (i.e. $\tau_1 \approx 0.20$ ns, $\tau_2 \approx 0.37$ ns, $I_2 \approx 0.60$, $\bar{\tau} \approx 0.30$ ns, $\tau_B \approx 0.28$ ns, $k_d \approx 1.4$ ns^{-1} and $\tau_1 \approx 0.225$ ns, $\tau_2 \approx 0.385$ ns, $I_2 \approx 0.50$, $\bar{\tau} \approx 0.30$ ns; $\tau_B \approx 0.285$ ns, $k_d \approx 0.9$ ns^{-1}, respectively), are obtained within two-state positron trapping model [22]. Here, optimal set of two-component fitting parameters calculated with LT computer program are selected. It should be noted that using of three-component and even more complicated models to interpret the PALS results obtained is not successful and ineffective due to high *FIT* values and limited resolution of experimental measurements.

The PALS results obtained regarding long-lived component $\tau_2 \approx 0.370$ ns, which is attributed to the defect-related lifetime associated with nanovoid volume, well agree with the reference data from, for example, K. Jensen et al. [17] for g-As_2Se_3. By using the linear dependence between numerical values of positron lifetimes τ (in ns) and vacancy volume V (in Å^3) (see Eq. 2), the magnitude of nanovoid volume corresponded to the $\tau_2 \approx 0.370$ ns is determined being equal to $V \approx 100$ Å^3 with nanovoid radius $r \approx 2.9$ Å. Because of the value of relative intensity I_2 is more than 50 %, the large concentration of nanovoids with $r \approx 2.9$ Å seems to be existed in the real structure of *g*-As_2Se_3.

The PALS data obtained are in a good agreement with Popescu's theoretical modelling of nanovoid topology for layer-biased (146 atoms) structure of *g*-As_2Se_3 using Monte-Carlo simulation [13]. It has been found within this modelling that nanovoid structure of *g*-As_2Se_3 includes at least three types of free-volume nanovoids centered near $\bar{r}_1 \approx 1.5$ Å, $\bar{r}_2 \approx 2.3$ Å and $\bar{r}_3 \approx 2.9$ Å (Fig. 3).

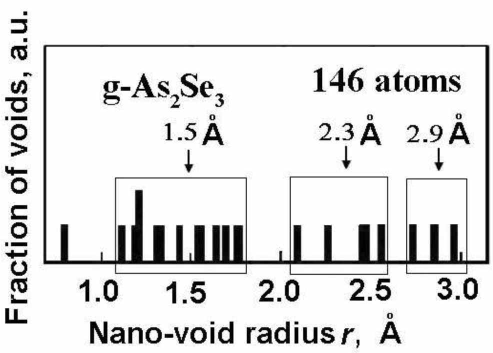

Fig. 3. Nanovoid distribution for layer-biased 146-atoms structural model of g-As_2Se_3 after M. A. Popescu [13].

In this respect, PALS data obtained can be explained as follows. The numerical value of the greatest nanovoids centred near $\bar{r}_3 \approx 2.9$ Å (Fig. 3) is in full agreement with the experimental results obtained using Eq. (2) for long-lived lifetime component $\tau_2 \approx 0.37$ ns, associated with the nanovoids of $V \approx 100$ Å^3 or $r \approx 2.9$ Å. From this reason another two types of nanovoids centered near $\bar{r}_1 \approx 1.5$ Å and $\bar{r}_2 \approx 2.3$ Å make contribution into short-lived lifetime component $\tau_1 \approx 0.20$ ns with obviously sufficiently low values of positron trapping rate k_d.

Following to the Elliott's void-based model for explanation of the FSDP origin [16] in the case of tetravalent AX_2 glasses, let's find the similar to Eq. (1) analytical relationship, connecting the position of the FSDP, Q_1, and diameter of free-volume nanovoids, D, for layer-like type investigated g-As_2Se_3.

Let's represent the Eq. (1) through coefficient k, depending on the type of glass structure, as

$$Q_1 = k \cdot \pi/D, \tag{9}$$

that is, $k = 1.5$ for tetravalent type structure of ChG. So, for layer-like (L) type of g-As_2Se_3 coefficient k should be estimated as

$$k = D^{L} \cdot Q_1^{L}/\pi. \tag{10}$$

According to Jensen et al. [17], the same nanovoids could bee responsible for the origin of the FSDP and trapping of positrons in glassy-like matrix. So, by suggesting that the nanovoids with radius $r \approx 2.9$ Å, existed in the real structure of g-As_2Se_3 from PALS results obtained and Popescu's theoretical modeling [13] (see Fig. 3), are also responsible for the nature of the FSDP and trapping of positrons in this material (i.e. $D^{L} \approx 5.8$ Å) and taken the experimental value of $Q_1^{L} = Q_{FSDP} \approx 1.25$ $Å^{-1}$ for g-As_2Se_3 (see Table 1), we can obtain the value of $k \approx 2.3$. Therefore, in the case of assumption made, the real relationship between the position of the FSDP and diameter of nanovoids for layer-like type g-As_2Se_3 should be written as:

$$Q_1 = Q_{FSDP} \approx 2.3\pi/D. \tag{11}$$

Of course, Eq. (11) obtained must be checked for another representative of layer-like type ChG such as g-As_2S_3. It will be the objective of our next research. Besides, it is very significant to conduct the experimental test for mixed layer-like and tetravalent type materials in order to understand better the structural features of glassy-like chalcogenides in various glass-forming configurations. So the main goals of the future research will be concentrated on the nanostructural characterization of binary As_2S_3, pseudo-binary As_2S_3-As_2Se_3 and ternary As(Sb)-Ge-S(Se) ChG widely used in optoelectronics.

4. Conclusions

In the present work, we have firstly demonstrated that the FSDP-related XRD method along with PALS technique can be adequate experimental tools to study nanostructural voids in glassy-like chalcogenide materials. Although, the results obtained only for g-As_2Se_3 cannot be directly applied for many others binary and multicomponent ChG, but the idea, firstly suggested by Jensen with co-workers [17], that the same nanovoids are responsible for the origin of the FSDP and trapping of positrons in glassy-like matrix seems to be reasonable in a general occurrence. The confirmation to this statement is found comparing the experimental PALS data obtained with Popescu's theoretical modelling [13] of nanovoids distribution in g-As_2Se_3 structure. In terms of this idea, it has been established that the coefficient k connecting the position of the FSDP with nanovoid diameter for the investigated layer-like g-As_2Se_3 equals 2.3, giving therefore the empirical Eq. (11). By comparing Eq. (1), adequately tested by Elliott for the FSDP in tetravalent ChG [11,15,16], with Eq. (11) obtained for layer-like type g-As_2Se_3, we can conclude that the real nanovoid structure in ChG is essentially dependent on dimensionality of glass network. In this respect, the further research of binary g-As_2S_3, pseudo-binary g-As_2S_3-As_2Se_3, and ternary g-As(Sb)-Ge-S(Se) compositions with different structural dimensionality will be very useful to develop the general model for various glassy-like chalcogenides.

Acknowledgements

This work was partially supported by a grant from the Fund of Fundamental Researches of Ministry of Education and Science of Ukraine (Project No 02.07/0042). T.K. is also acknowledged a grant by the Mianowski Fund (Poland). Special thanks to Dr. J. Filipecki and Dr. A. Kozdras for their assistant in positron annihilation measurements and interpretation of PALS data and Prof. M. Popescu for his interest to this work and useful discussions.

References

[1] A. Feltz, Amorphous and Vitreous Inorganic Solids, Mir, Moscow, 1986 (in Russian).
[2] J. Savage, J. Non-Cryst. Solids **47**, 101 (1982).
[3] A. Feltz, W. Burckhardt, B. Voight , D. Linke , J. Non-Cryst. Solids **129**, 31 (1991).
[4] A. Seddon, J. Non-Cryst. Solids **184**, 44 (1995).
[5] J.-L. Adam, J. Non-Cryst. Solids **287**, 401 (2001).
[6] S. Onari, T. Inokuma, H. Kataura, T. Arai, Phys. Rev. **B 35** (9), 4373 (1987).
[7] Ya. A. Teteris, M. Ya. Rejnfelde, Izv. AN SSSR. Neorgan. Mater. **22** (4), 584 (1986) (in Russian).
[8] I. P. Kotsalas, D. Papadimitriou, C. Raptis, M. Vlcek, M. Frumar, J. Non-Cryst. Solids **226**, 85 (1998).
[9] O. I. Shpotyuk, R.Ya. Golovchak, T. S. Kavetsky, A. P. Kovalskiy, M. M. Vakiv, Nucl. Instr. Meth. Phys. Res. **B 166-167**, 517 (2000).
[10] S. Kokenyesi, J. Csikai, P. Raics, I. A. Szabo, S. Szegedi, A. Vitez, J. Non-Cryst. Solids **326&327**, 209 (2003).
[11] S. R. Elliott, Nature **354**, 445 (1991).
[12] M. Kastner, Phys. Rev. **B 7**, 5237 (1973).
[13] M. A. Popescu, J. Non-Cryst. Solids **35-36**, 549 (1980).
[14] S. G. Bishop, N.J. Shevchik, Solid State Commun. **15**, 629 (1974).
[15] S. R. Elliott, Phys. Rev. Lett. **67**, 711 (1991).
[16] S. R. Elliott, J. Non-Cryst. Solids **182**, 40 (1995).
[17] K. O. Jensen, P. S. Salmon, I. T. Penfold, P. G. Coleman, J. Non-Cryst. Solids **170,** 57 (1994).
[18] S. Hosokawa, Y. Kawakita, W. -C. Pilgrim, F. Hensel, J. Non-Cryst. Solids **293-295,** 153 (2001).
[19] P. H. Gaskell, J. Non-Cryst. Solids **351**, 1003 (2005).
[20] M. Popescu, F. Sava, A. Lőrinczi, J. Optoelectron. Adv. Mater. **6**(3), 887 (2004).
[21] M. Popescu, J. Optoelectron. Adv. Mater. **6**(4), 1147 (2004).
[22] A. Kozdras, J. Filipecki, M. Hyla, O. Shpotyuk, A. Kovalskiy, S. Szymura, J. Non-Cryst. Solids **351**, 1077 (2005).
[23] J. Kansy, Nucl. Instr. Meth. Phys. Res. **A 374,** 235 (1996).
[24] M. J. Puska, C. Corbel, R. M. Nieminen, Phys. Rev. **B 41**, 9980 (1990).